

Recent Advances in Solid-State White Light-Emitting Electrochemical Cells

Hai-Ching Su* and Chia-Yu Cheng^[a]

Abstract: Compared to organic light-emitting diodes, solid-state light-emitting electrochemical cells (LECs) exhibit advantages of simple device structures, low operation voltages, and compatibility with air-stable metal electrodes. Since the first demonstration of white LECs in 1997, the cells have been studied extensively, due to their potential ap-

plications in solid-state lighting. This article reviews the development of white LECs based on conjugated polymers and cationic transition metal complexes. Important achievements of each work on white LECs are highlighted. Finally, the outlook for future development of white LECs is discussed.

Keywords: electrochemistry · light-emitting electrochemical cells · organic light-emitting devices · polymers

1 Introduction

Recently, white organic light-emitting diodes (OLEDs) have received considerable attention owing to their potential applications in flat panel displays and solid-state lighting.^[1–5] However, sophisticated multilayered device structures complicate fabrication processes and increase costs, influencing their competitiveness with other white light-emitting technologies. Compared with conventional OLEDs, solid-state light-emitting electrochemical cells (LECs)^[6,7] have several promising advantages. Solid-state LEC devices generally require only a single emissive layer, which can be easily fabricated by solution processes. The emissive layers of LECs contain mobile ions, which can drift toward electrodes under an applied bias. The spatially separated mobile ions induce electrochemical doping (oxidation and reduction) of the emissive materials near the electrodes (i.e., p-type and n-type doping near the anode and cathode, respectively).^[7] The electrochemically doped regions form ohmic contacts with the electrodes and, consequently, facilitate the carrier injection, which recombines at the intrinsic layer between p- and n-type regions.^[8] Typically, a single-layered LEC device can be operated at low voltages (close to E_g/e , where E_g is the energy gap of the emissive material and e is elementary charge) with balanced carrier injection, giving high power efficiencies (lm W^{-1}). Furthermore, air-stable metals (e.g., gold and silver) can be used as electrodes, since carrier injection in LECs is relatively insensitive to work functions of electrode materials. Therefore, LECs are good candidates for white light-emitting sources.

Solid-state LECs can be roughly divided into two categories, according to the emissive materials used. The first type of material is fluorescent conjugated light-emitting

polymers.^[6,7,9–19] In these LECs, the emissive layers contain ionic salts for providing mobile ions. In addition, ion-conducting polymers (e.g., poly[ethylene oxide] [PEO]) are incorporated, to avoid phase separation between non-polar conjugated light-emitting polymers and polar salts. The second type of LEC is relatively simpler, since only single-component cationic transition metal complexes (CTMCs) are utilized as the emissive materials.^[20–45] No ion-conducting material is needed in CTMC-based LECs, since CTMCs are intrinsically ionic. Furthermore, electroluminescence (EL) efficiencies of CTMC-based LECs are generally higher, due to the phosphorescent nature of CTMCs. Since the first white LECs (WLECs) were reported by Yang et al. in 1997,^[46] WLECs based on fluorescent conjugated light-emitting polymers and phosphorescent CTMCs have been intensively studied, and device efficiencies have been significantly enhanced. This review illustrates previous development of WLECs and highlights important achievements and technical challenges for further improving device performance of WLECs.

[a] H.-C. Su, C.-Y. Cheng
Institute of Lighting and Energy Photonics
National Chiao Tung University
No. 301, Gaofa 3rd Road
Guiren District
Tainan 71150 (Taiwan)
Tel: (+886) 6-3032121-57792
Fax: (+886) 6-3032535
e-mail: haichingsu@mail.nctu.edu.tw

2 Fluorescent WLECs

2.1 WLECs Based on Phase Separation and Excimers

The first WLECs were demonstrated by incorporating a small amount of PEO in the emissive layers based on poly[9,9-bis(3,6-dioxaheptyl)-fluorene-2,7-diyl] (**P1**).^[46] **P1** is an efficient blue-green-emitting material and exhibits a high photoluminescence quantum yield (PLQY) of 73% photon/photon in neat films. The polyether-type side groups of **P1** (Figure 1) were designed to promote the ionic conductivity necessary for LEC operation. Blue-

green LECs based on a blend of **P1** and LiCF₃SO₃ showed an external quantum efficiency (EQE) of 4% photons/electron and a power efficiency of 12 lmW⁻¹ at 3.1 V. When PEO was additionally blended into the emissive layer, phase separation between **P1** and PEO took place and the EL emission became white. The WLECs based on phase separation exhibited a lowered EQE of 2.4% and brightness of 400 cdm⁻² under 4 V (Table 1). The reduced device efficiency may result from an emissive layer that is foggy and opaque due to phase separation. The EL emission of these WLECs showed a maximum at ca. 550 nm, and the intensity of the blue and red

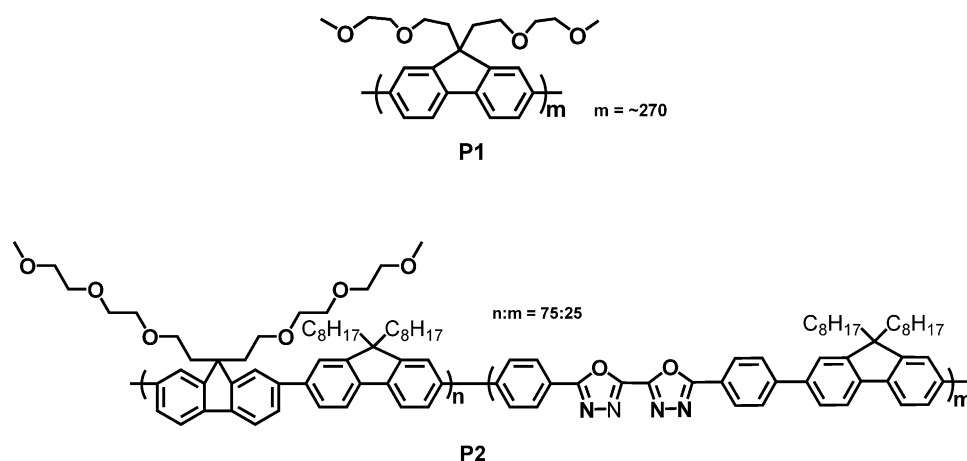


Figure 1. Molecular structures of the light-emitting polymers used for WLECs based on phase separation and excimers.

Hai-Ching Su obtained his B.S., M.S., and Ph.D. degrees from the National Taiwan University, Taipei, Taiwan in 2001, 2003, and 2007, respectively. In 2009, he joined the National Chiao Tung University, where he is currently an associate professor. His research interests concern white light-emitting electrochemical cells (LECs) and issues of adjusting carrier balance of LECs. He was awarded the Thomson Reuters Taiwan Research Front Award in 2011.



Chia-Yu Cheng received her B.S. degree in physics from the Chung Yuan Christian University in 2013. Then, she joined Prof. Hai-Ching Su's group in pursuit of her M.S. degree. Her research interests are focused on microcavity effects in tandem LECs.



emission was significantly lower than that of the central yellow emission. The shift of EL emission of the LECs containing PEO most likely also results from the phase separation in the blend emissive layer and the consequent change of the stacking pattern of the **P1** polymer chains. This pioneering work opened a new way to obtain white EL under low biases and initiated the development of WLECs in the following two decades.

Based on a similar concept, combination of EL emission from individual polymer chains and excimers can also generate white light from LECs. In 2010, Sun et al. reported WLECs based on a fluorene-oxadiazole copolymer.^[47] This copolymer has a π -conjugated backbone consisting of 75 mol% fluorene and 25 mol% 5,5'-diphenyl-2,2'-bi-1,3,4-oxadiazole (**P2**, Figure 1). 2-(2-(2-Methoxyethoxy)ethoxy)ethyl, attached to C-9 of the fluorenes, was introduced to enhance ionic conductivity necessary for LEC operation. Polymer **P2** showed deep blue photoluminescence (PL) in tetrahydrofuran solutions and in neat films. The EL emission spectrum of polymer light-emitting diodes (PLEDs) based on **P2** resembled the PL spectrum of **P2**. However, the EL spectrum of the LEC devices containing **P2** and LiCF₃SO₃ exhibited intense emission in the green and red spectral regions, rendering

Table 1. Summary of EL characteristics of WLECs

Emissive layer ^[a]	Bias (V)	J (mA cm ⁻²) ^[b]	CIE (x, y) ^[c]	CR ^[d]	t _{max} (min) ^[e]	L _{max} (cd m ⁻²) ^[f]	η _{ext, max} , η _{L, max} , η _{p, max} (%), cd A ⁻¹ , lm W ⁻¹) ^[g]	t _{1/2} (min) ^[h]
P1 , PEO, LiCF ₃ SO ₃ (10:1:2) ^[i] [46]	4 ^[i]	–	–	–	–	400	(2.4, –, –)	–
P2 , LiCF ₃ SO ₃ (5.2–5.6:1) ^[i] [47]	6.4 ^[k]	–	(0.24, 0.31)	–	–	257	(–, 0.15, –)	–
P3B, P3G, P3R , TMPE, LiCF ₃ SO ₃ (100:1:3:10.4:3.12) ^[i] [48]	–	7.7 ^[l]	(0.39, 0.43)	83	ca. 180	ca. 240	(–, 3.1, 1.6)	ca. 720
P4 [50]	3 ^[i]	–	(0.36, 0.38)	72	17	13	(0.69, –, 1.56)	36
	3.3 ^[i]	–	(0.30, 0.34)	72	8	113	(0.66, –, 1.28)	13
	3.5 ^[i]	–	(0.31, 0.34)	71	5	231	(0.55, –, 0.95)	7
P5 , TMPE, LiCF ₃ SO ₃ (100:10:3) ^[i] [51]	–	5.7 ^[l]	(0.41, 0.45)	82	> 360	> 200	(–, 3.8, 1.2)	–
C1B , BMIMPF ₆ , C1R (80.5:19.1:0.4) ^[i] [52]	2.9 ^[i]	–	(0.45, 0.40)	81	240	2.5	(4.0, 7.2, 7.8)	534
	3.1 ^[i]	–	(0.37, 0.39)	80	60	18	(3.4, 6.1, 6.2)	78
	3.3 ^[i]	–	(0.35, 0.39)	80	30	43	(3.3, 5.8, 5.5)	24
C2B , BMIMPF ₆ , C2R (100:35:0.4) ^[m] [53]	4 ^[i]	–	(0.45, 0.44)	81	ca. 100	106	(4.7, 9.8, –)	ca. 450
C2B , BMIMPF ₆ , C2R (100:35:0.2) ^[m] [53]	4 ^[i]	–	(0.40, 0.45)	80	ca. 100	115	(4.4, 9.5, –)	ca. 300
	3.5 ^[i]	–	(0.42, 0.44)	81	–	31	(5.2, 11.2, 10)	–
C3B , BMIMPF ₆ , C2R (100:100:0.8) ^[m] [54]	3.2 ^[i]	–	(0.37, 0.41)	80	ca. 25	7.9	(5.6, 11.4, 11.2)	ca. 50
C4B , BMIMPF ₆ , C4R (100:10:1) ^[i] [55]	3.5 ^[i]	–	–	–	68	31	(4.5, 11.1, –)	–
	4 ^[i]	–	–	–	28	116	(5, 12.4, –)	–
	4.5 ^[i]	–	–	–	11	281	(3.4, 8.5, –)	–
C5B , BMIMPF ₆ , C1R , C5O (79.85:20:0.05:0.1) ^[i] [59]	2.9 ^[i]	–	(0.53, 0.44)	84	280	1.2	(5.6, 9.2, 10)	446 ^[n]
	3.1 ^[i]	–	(0.37, 0.45)	75	60	11.5	(7.4, 14.8, 15)	120
	3.3 ^[i]	–	(0.32, 0.43)	70	29	20.2	(6.3, 13.4, 12.8)	37
C5B : BMIMPF ₆ : C1R (79.85:20:0.15) ^[i] [64]	3.1 ^[i]	–	(0.37, 0.40)	77	250	1.8	(11.1, 17.6, 17.4)	110
	3.3 ^[i]	–	(0.32, 0.39)	74	112	5.7	(10.7, 18.6, 19.5)	89
	3.5 ^[i]	–	(0.30, 0.38)	73	77	9.9	(10.4, 19.5, 17.5)	57
C5B : BMIMPF ₆ (80:20) ^[i] CCL (PMMA:DC)TB (99.6:0.4) ^[i] [60]	3.1 ^[i]	–	–	–	129	2.9	(5.9, –, 15.3)	111
	3.3 ^[i]	–	(0.37, 0.44)	66	103	9.5	(5.5, –, 13.4)	47
	3.5 ^[i]	–	–	–	66	16.2	(5.5, –, 12.7)	23
C5B : BMIMPF ₆ : SR101 (79.7:20:0.3) ^[i] [71]	3.6 ^[i]	–	(0.32, 0.30)	72	90	12.6	(7.5, –, 13.7)	120
	3.8 ^[i]	–	(0.30, 0.31)	73	60	19.4	(7.9, –, 15.6)	90

[a] Components of the emissive layer and the references of the data. [b] Current density. [c] CIE 1931 chromaticity coordinates. [d] Color rendering index. [e] Time required to reach maximum brightness. [f] Maximum brightness. [g] Maximum external quantum efficiency, current efficiency, and power efficiency. [h] Time for the brightness of the device to decay from the maximum to half of the maximum. [i] Mass ratios. [j] Under constant bias voltage. [k] Voltage at maximum current efficiency. [l] Under constant current density. [m] Molar ratios. [n] Extrapolated.

a white EL spectrum with a full width at half-maximum of 160 nm. The green and red emission may result from excimers formed when the ionic species are present. The EL characteristics of WLECs based on **P2** are summarized in Table 1. This work is the first demonstration of WLECs employing a single polymer in the emissive layer.

2.2 Trichromatic Host-Guest WLECs

It is difficult to tailor the EL spectra of WLECs based on phase separation and excimers to achieve high-quality white light for applications. To obtain white EL with good color rendering properties, in 2011, Tang et al. reported trichromatic WLECs based on blue, green, and red-emitting polyspirobifluorene-based copolymers (**P3B**, **P3G**, and **P3R**, Figure 2).^[48] The ion-transport material trimethylolpropane ethoxylate (TMPE) and the salt LiCF_3SO_3 were mixed as the electrolyte in the emissive layer. White EL spectra can be easily tailored by adjusting the mixing ratios of blue, green, and red copolymers. With an optimized mixing mass ratio (**P3B**:**P3G**:**P3R** = 100:1:3), white EL spectra with Commission Internationale de l'Éclairage (CIE) coordinates (0.39, 0.43) and a color rendering index (CRI) value of 83 were obtained. The peak current efficiency and power efficiency achieved in these optimized WLECs were 3.1 cdA^{-1} and 1.6 lmW^{-1} , respectively. It is noted that polyspirobifluorene-based copolymers exhibited superior electrical stability and, thus, long device lifetimes, which are defined as the time it takes for the brightness of the device to decay from the maximum to half of the maximum; device lifetimes of up to 12 hours were measured for these WLECs. This work was the first demonstration of polymer WLECs employing the host-guest strategy.^[30,34,49]

2.3 Single-Component Multiple-Chromophore WLECs

In comparison to multiple-component WLECs, single-component WLECs require relatively easier fabrication processes. In 2013, Tsai et al. reported single-component WLECs based on a fluorene-benzoselenadiazole copolymer (**P4**, Figure 3).^[50] Polymer **P4** is composed of a blue-emitting polyfluorene (PF) main chain incorporated with yellow-emitting 2,1,3-benzoselenadiazole moieties (0.25%). The PL of thin films of **P4** dispersed in poly(methyl methacrylate) (PMMA) showed clear emission bands around 560 nm even when the doping concentration of **P4** was low (1%). Thus, the yellow emission band results from the presence of 2,1,3-benzoselenadiazole along the PF main chain and is not related to aggregates of fluorene segments. The WLECs based on **P4** showed bias-dependent EL spectra. At a lower bias, carrier injection and trapping on the smaller-gap 2,1,3-benzoselenadiazole was favored and, thus, direct exciton formation on the lower-gap chromophore led to more significant yellow emission (Figure 4a). When the bias was increased, carrier injection and exciton formation on the higher-gap fluorene was facilitated, and subsequent partial energy transfer dominated the yellow emission, resulting in less significant yellow emission (Figure 4a). The emissive layer thickness also affects the EL spectra of WLECs. A lower electric field in a thicker device impedes carrier injection onto the higher-gap fluorene, and thus, direct exciton formation on the lower-gap chromophore is preferred, resulting in more significant yellow emission (Figure 4b). In contrast, a higher electric field in a thinner device facilitates carrier injection onto the higher-gap fluorene. Yellow emission results mainly from partial energy transfer from blue excitons on the fluorene, and thus, re-

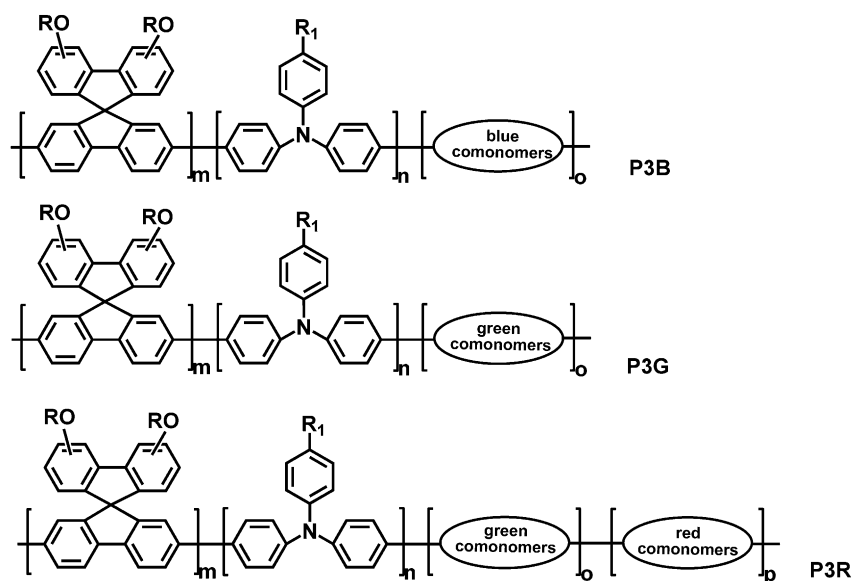


Figure 2. Molecular structures of the blue, green, and red light-emitting copolymers used for trichromatic WLECs.

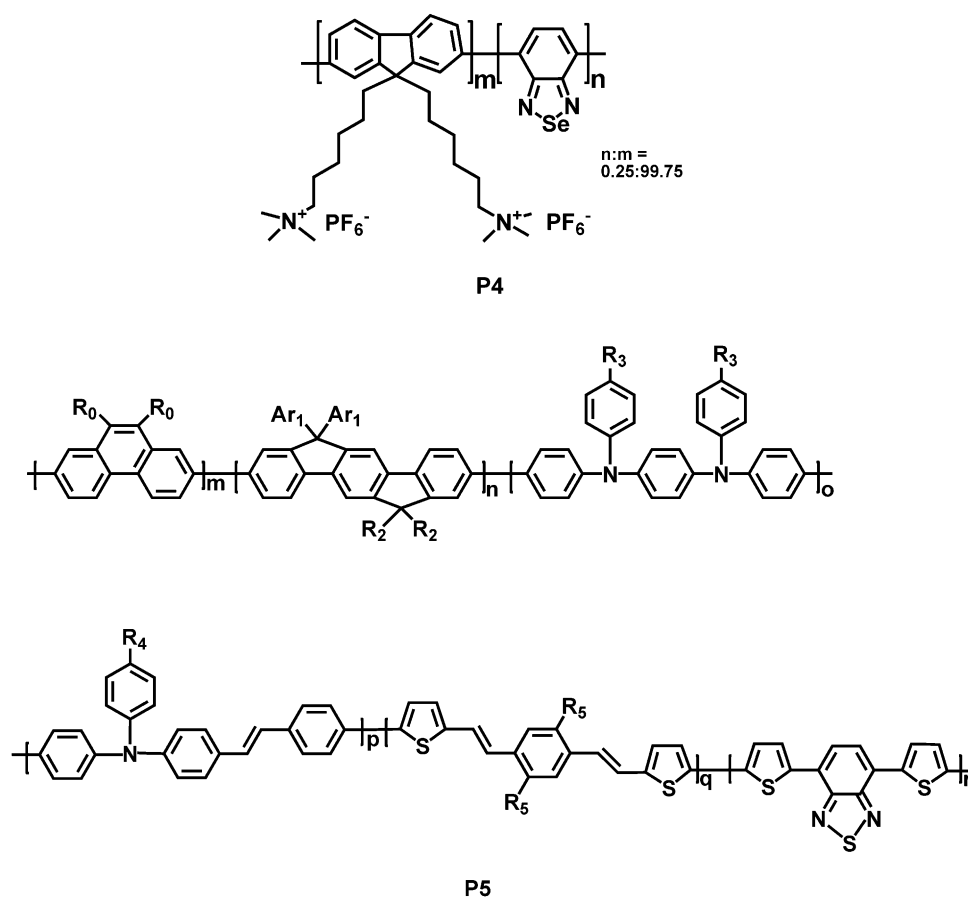


Figure 3. Molecular structures of the light-emitting copolymers used for single-component, multiple-chromophore WLECs.

duced yellow emission is present (Figure 4b). As a result, the EL spectrum of single-component multiple-chromophore WLECs can be tailored by adjusting the bias and/or the thickness of the emissive layer. The peak EQE and power efficiency achieved in WLECs based on **P4** are 0.69% and 1.56 lm W^{-1} , respectively.

An alternative way to achieve white EL emission from LECs is to impede energy transfer between the blue-emitting and red-emitting chromophores in multiple-chromophore copolymers. In 2013, Tang et al. proposed a multifluorophoric conjugated copolymer (**P5**, Figure 3) and an electrolyte designed to inhibit energy-transfer interactions and, thus, to obtain white EL from WLECs based on these mixtures.^[51] The OLEDs containing **P5** without electrolytes and salts, which provide mobile ions, showed narrow-band red emission. This result reveals that polymer chains of **P5** are in the aggregated state and that the excitons created on the higher-energy blue and green chromophores are funneled to the lower-energy red chromophores via efficient energy transfer. However, polymer chains of **P5** would be efficiently separated if LiCF_3SO_3 -TMPE electrolytes were added in the emissive layer, and the energy transfer rate would be reduced. Hence, some residual blue emission took place, along with red emis-

sion, and the WLECs based on **P5** and LiCF_3SO_3 -TMPE electrolytes exhibited white EL spectra with CIE coordinates (0.41, 0.45) and a CRI value of 82. Notably, the white EL spectrum was unchanged across a wide current density range (5.7 – 46.2 mA cm^{-2}). This is an important feature for practical solid-state lighting applications.

3 Phosphorescent WLECs

3.1 Dichromatic WLECs

The above mentioned studies of fluorescent solid-state white LECs based on conjugated light-emitting polymers generally showed moderate EL efficiencies, due to the limitation of fluorescent spin statistics. To improve device efficiencies, in 2008, Su et al. reported the first WLECs based on phosphorescent CTMCs.^[52] By employing a blue-emitting host complex (**C1B**, Figure 5) and a red-emitting guest complex (**C1R**, Figure 6), the host-guest WLECs showed a high EQE of 4% and power efficiency of 7.8 lm W^{-1} (Table 1). Since the LECs based on CTMCs showed slow device response, the ionic liquid 1-butyl-3-methylimidazolium hexafluorophosphate [$\text{BMIM}^+(\text{PF}_6^-)$] was added to the emissive layer to provide additional

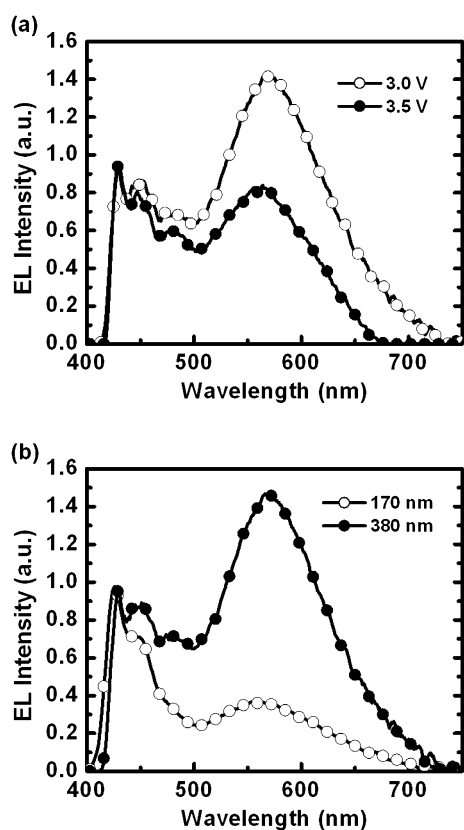


Figure 4. Comparison of EL spectra of WLECs based on **P4** (a) under different bias voltages (3 and 3.5 V), at constant emissive layer thickness (370 nm) and (b) for different emissive layer thicknesses (170 and 380 nm), under constant bias voltage (3 V).

anions, which shortened the device response time.^[32] The host-guest WLECs based on **C1B** and **C1R** also showed bias-dependent EL spectra. As shown in Figure 7, the red emission increased relative to the blue emission, as the bias decreased. This increase could be caused by energy level alignments of the host **C1B** and guest **C1R** (inset of Figure 7). At a lower bias, such energy level alignments prefer carrier injection and trapping on the lower-gap guest, resulting in direct carrier recombination and exciton formation on the guest. Therefore, a larger fraction of guest emission was observed at a lower bias. When a higher bias is applied, carrier injection onto the higher-gap host is facilitated, and the guest emission comes mainly from subsequent host-guest energy transfer, rendering a reduced fraction of guest emission. This first demonstration of WLECs based on CTMCs boosted significant enhancement in device efficiencies of WLECs achieved by several groups in the following few years.

Based on the same concept, in 2009, He et al. reported WLECs employing blue-emitting host **C2B** (Figure 5) doped with red-emitting host **C2R** (Figure 6).^[53] When biased at 3.5 V, the WLECs containing **C2B**, BMIMPF_6 , and **C2R** (molar ratio = 100:35:0.2) had a peak EQE, current efficiency, and power efficiency of 5.2%, 11.2 cd A^{-1} , and 10 lm W^{-1} , respectively. These WLECs also exhibited white EL spectra with CIE coordinates (0.42, 0.44) and CRI values up to 81. To further enhance device efficiencies of WLECs, the same group proposed a blue-emitting CTMC, **C3B** (Figure 5), with the sterically bulky 4-tritylphenyl group on the ancillary ligand, which

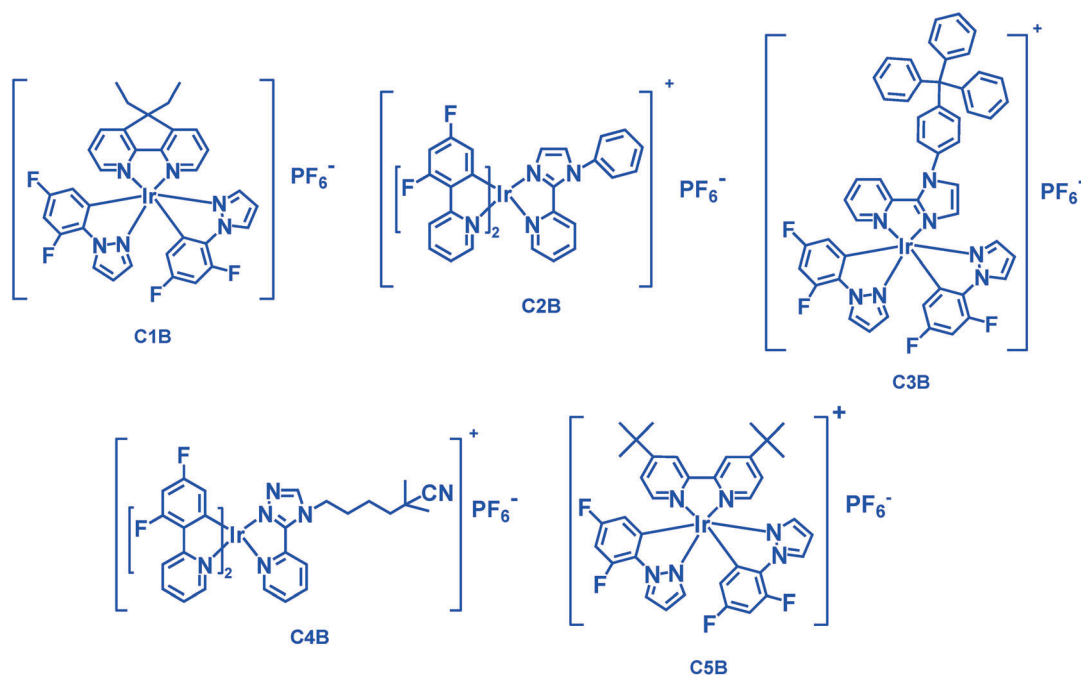


Figure 5. Molecular structures of blue-emitting CTMCs used in WLECs.

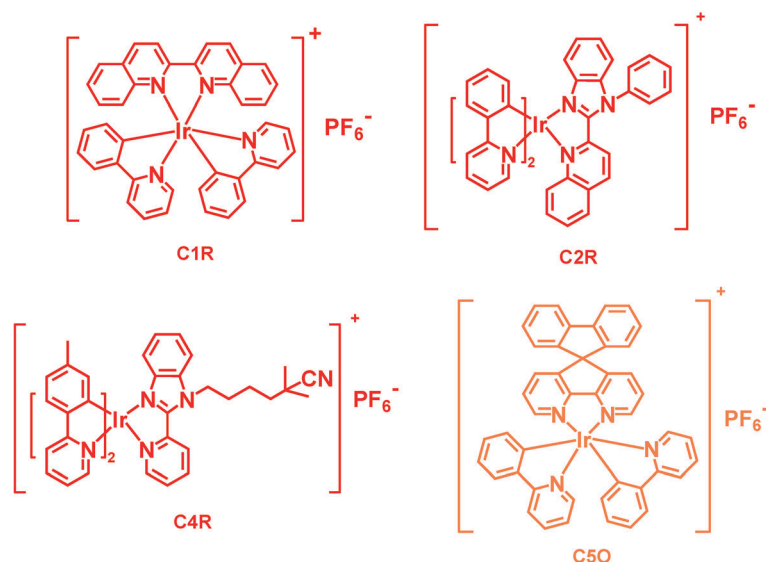


Figure 6. Molecular structures of red and orange-emitting CTMCs used in WLECs.

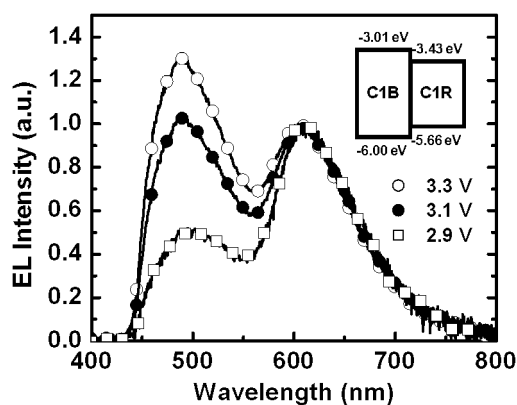


Figure 7. Bias-dependent EL spectra of WLECs (mass ratio $\text{C1B}:\text{BMIMPF}_6:\text{C1R}=80.5:19.1:0.4$). Inset: energy level diagram of **C1B** and **C1R**.

reduces the intermolecular interactions and excited-state self-quenching of **C3B** in neat films.^[54] Therefore, complex **C3B** showed high PLQYs of 54 and 67% in neat films and in thin films mixed with BMIMPF_6 (molar ratio = 1:1), respectively. The peak EQE, current efficiency, and power efficiency of the WLECs containing **C3B**, BMIMPF_6 , and **C2R** (molar ratio = 100:100:0.8) reached 5.6%, 11.4 cd A^{-1} , and 11.2 lm W^{-1} , respectively. These works successfully illustrated improvement of WLEC device efficiencies via proper design of molecular structures of CTMCs.

Recently, Chen et al. proposed WLECs based on a higher-gap host, **C4B** (Figure 5), and a lower-gap guest, **C4R** (Figure 6).^[55] The peak EQE and current efficiency reached in the WLECs containing **C4B**, BMIMPF_6 , and **C4R** (mass ratio = 100:10:1) were 5% and 12.4 cd A^{-1} , respectively, which are similar to those obtained for previ-

ously reported dichromatic WLECs based on host-guest CTMCs.^[52–54] These results imply that improvements to CTMCs alone are not sufficient to further enhance device efficiencies of WLECs. Device engineering for improving carrier balance is required to optimize device performance of WLECs.

3.2 WLECs with Improved Carrier Balance

Adjusting carrier balance has a significant effect on host-guest LECs,^[40,56–58] since offsets in energy levels of host and guest molecules induce carrier trapping, and variation of the doping concentrations of guests alters the balance of carrier mobilities of the host films. Balanced electron and hole mobilities would be beneficial for keeping the recombination zone near the center of the emissive layer and, thus, would prevent exciton quenching and enhance the device efficiency. In 2011, Su et al. reported adjusting the carrier balance of host-guest WLECs to improve device efficiencies by employing a double-doped strategy.^[59] The blue-emitting CTMC used in this work (**C5B**, Figure 5) has been reported by Tamayo et al.,^[31] and the red-emitting CTMC is the same one used in the first demonstration of WLECs based on CTMCs^[52] (**C1R**, Figure 6). Complex **C5B** shows approximately the same PL spectra in solution as in neat films, likely due to reduced intermolecular interactions in the presence of the sterically bulky di-*tert*-butyl groups of the bipyridine ligand.^[31] Highly retained PLOQY of **C5B** in neat films (75%), in comparison to that in solution (100%), further confirms the reduced self-quenching in neat films due to the sterically bulky ligand, suggesting **C5B** is suitable for use as the host of WLECs.^[59] The blue-emitting LECs based on **C5B** exhibited high EQEs, up to 14.5%.^[60] These efficiencies reveal superior carrier balance in the

C5B host films, compared to the maximal EQE achievable in devices with the typical layered light-emitting structure, for which PLQY is 75% and optical outcoupling efficiency is ca. 20%. However, the single-doped WLECs (mass ratio **C5B**:BMIMPF₆:**C1R** = 79.8:20:0.2) showed low EQEs of 3.2%, in spite of the high PLQY of the emissive layer (61%).^[59] As the energy levels in Figure 8

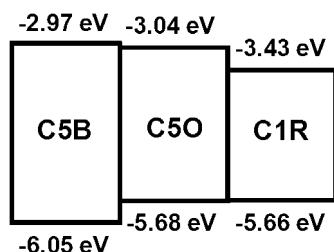


Figure 8. Energy level diagram of **C5B**, **C5O**, and **C1R**.

show, the single-doped emissive layer has a slightly larger energy offset between host (**C5B**) and guest (**C1R**) in the lowest unoccupied molecular orbital (LUMO) levels (0.46 eV) than it does in the highest occupied molecular orbital (HOMO) levels (0.39 eV). This may lead to more pronounced electron trapping and, thus, deterioration of carrier balance in the host-guest films. If an orange guest (**C5O**, Figure 6) with a higher LUMO level (Figure 8) is incorporated to reduce electron trapping, carrier balance improves. The double-doped WLECs (mass ratio **C5B**:BMIMPF₆:**C1R**:**C5O** = 79.85:20:0.05:0.1) showed high EQEs and power efficiencies, up to 7.4% and 15 lm W⁻¹, respectively (Table 1). These results confirm that the double-doping strategy is a useful technique for realizing highly efficient WLECs.

Since carrier balance is critical in optimizing device efficiencies of WLECs, technology for providing direct evidence of altered carrier balance is highly desired. Recently, Wang et al. propose a novel technique to dynamically probe the position of the temporal recombination zone of sandwiched LECs by utilizing the microcavity effect.^[61] Microcavity structures of sandwiched LEC devices modify wavelength-dependent optical outcoupling efficiencies^[62] and, thus, result in tailored EL spectra when the recombination zone is moving in the emissive layer. Therefore, the recombination zone positions of sandwiched LECs can be estimated by fitting measured EL spectra to simulated EL spectra based on the microcavity effect and properly adjusted emitting zone positions. The equation used for simulation is shown below.^[62]

$$|E_{\text{ext}}(\lambda)|^2 = \frac{T_2 \frac{1}{N} \sum_{i=1}^N \left[1 + R_1 + 2\sqrt{R_1} \cos\left(\frac{4\pi z_i}{\lambda} + \varphi_1\right) \right]}{1 + R_1 R_2 - 2\sqrt{R_1 R_2} \cos\left(\frac{4\pi L}{\lambda} + \varphi_1 + \varphi_2\right)} \times |E_{\text{int}}(\lambda)|^2$$

Here, R_1 and R_2 are the reflectances from the cathode and from the glass substrate, respectively; φ_1 and φ_2 are the phase changes on reflection from the cathode and from the glass substrate, respectively; T_2 is the transmittance from the glass substrate; L is the total optical thickness of the cavity layers; $|E_{\text{int}}(\lambda)|^2$ is the emission spectrum of the organic materials without incorporation of the microcavity effect; $|E_{\text{ext}}(\lambda)|^2$ is the output emission spectrum from the glass substrate; and z_i is the optical distance between the emitting sublayer i and the cathode. The emitting layer is divided into N sublayers, and their contributions are summed up. Since the width of the p-n junction was estimated—by capacitance measurements, when p- and n-type layers were fully established—to be ca. 10% of the thickness of the active layer of LECs,^[63] the width of the emitting layer is estimated to be one tenth of the thickness of active layer. A thickness of 1 nm for each emitting sublayer was used, and thus, $N = \text{thickness of the active layer}/10$. The PL spectrum of a thin film of the emissive layer of WLECs coated on a quartz substrate was used as the emission spectrum, without incorporation of the microcavity effect, since no highly reflective metal layer is present in this sample. With this tool, Jhang et al. studied the effects of emissive layer thickness on carrier balance and device efficiencies of WLECs (mass ratio **C5B**:BMIMPF₆:**C1R** = 79.85:20:0.15).^[64] As shown in Figure 9a, for a thinner WLEC (190 nm), the stabilized recombination zone was relatively closer to the anode, and exciton quenching near the p-type doped layer reduces device efficiencies. Therefore, a moderate EQE (7.5%), which is comparable to that of previously reported WLECs based on the same emissive materials with similar thicknesses,^[59] was obtained. Increasing the emissive layer thickness ensured enough spacing between the recombination zone and the doped layers, resulting in mitigated exciton quenching and improved device efficiencies. The stabilized recombination zone of WLECs with a thicker emissive layer (270 nm) was close to the center of the emissive layer (Figure 9b), and consequently, the peak EQE and the power efficiency were enhanced to ca. 11% and 20 lm/W, respectively (Table 1). These device efficiencies are the highest values among reported WLECs. Further increasing the emissive layer thickness resulted in an asymmetric recombination zone position (Figure 9c), possibly due to deteriorated balance of carrier mobilities under a lowered electric field. Exciton quenching near the p-type doped layer took place, as well, and significantly deteriorated EQEs (<5%) were measured. This work demonstrates that device efficiencies of WLECs can be significantly improved by adjusting the emissive layer thickness to avoid exciton quenching near the doped layers.

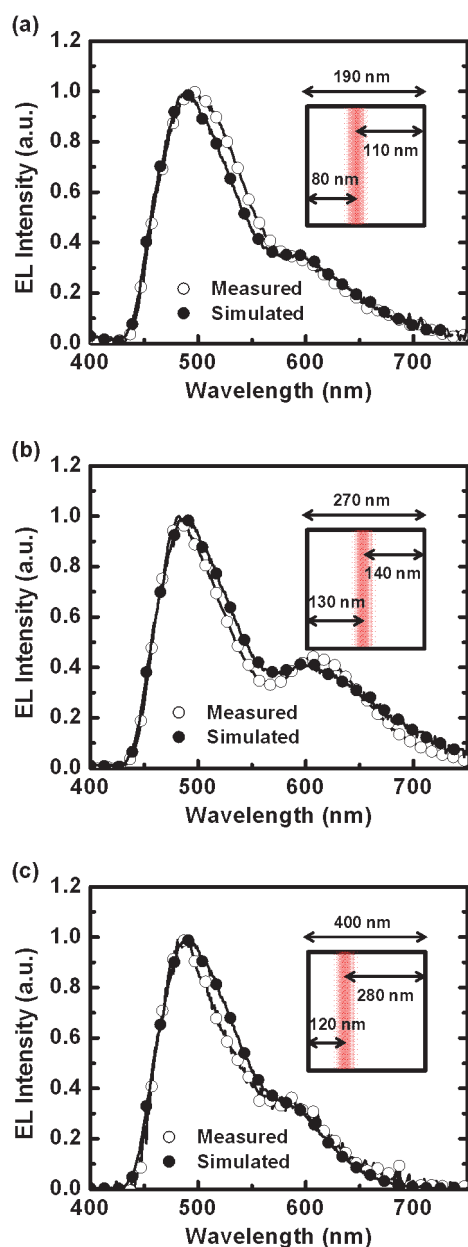


Figure 9. Simulated (solid circles) and measured (open circles) stabilized EL spectra of WLECs (mass ratio **C5B**:**BMIMPF₆**:**C1R** = 79.85:20:0.15) with emissive layer thicknesses (a) 190, (b) 270, and (c) 400 nm. The recombination zone position estimated from fitting of simulated and measured EL spectra is shown in the inset of each subfigure.

4 Fluorescent and Phosphorescent Hybrid WLECs

4.1 WLECs Employing Color Conversion Layers

Single-layered host-guest WLECs usually suffer bias-dependent color shifts (cf. Figure 7), which are undesired for practical applications.^[52–55,59,64] This phenomenon is attributed to excitons formed by direct carrier trapping on

the guest, under relatively lower biases, due to significant energy offsets in the energy levels between the host and the guest. Direct exciton formation on the lower-gap guest, due to charge trapping, dominates EL emission under lower biases, while exciton formation on the higher-gap host, followed by host-guest energy transfer, tends to be more significant under higher biases. Hence, the EL emission of the single-layered host-guest WLECs typically changes from red to white as the bias slightly increases. Color stability under varying bias conditions is also a critical issue in white OLEDs, and the combination of blue-emitting devices with red color conversion layers (CCLs) was reported to reach stable white EL.^[65] This approach can be implemented by easy fabrication techniques and can provide better color stability, since only one emitter is present in the emissive layer, eliminating the carrier trapping effect induced by the low-gap red-emitting dye. Based on the same concept, Wu et al. demonstrated color-stable WLECs by combining single-layered blue-emitting LECs with red-emitting CCLs on the inverse side of the glass substrate.^[60] The device structure is schematically shown in Figure 10. The emissive layer of

Ag
C5B/BMIMPF₆
PEDOT:PSS
ITO
Glass
Cover slip
CCL

Figure 10. Schematic diagram of the device structure of a WLEC employing a CCL.

the blue-emitting LECs is composed of **C5B** and **BMIMPF₆** (mass ratio 80:20), and the CCL is a thick (6 μm) PMMA film doped with 0.4 wt.% 4-(dicyanomethylene)-2-*t*-butyl-6-(1,1,7,7-tetramethyljulolidyl-9-enyl)-4H-pyran (**DCJTb**). The EL spectra of WLECs employing red CCLs were approximately the same under biases of 3.1 to 9.0 V, which correspond to device current densities and maximum brightnesses of 0.04 to 16.17 mA cm⁻² and 2.87 to 184.92 cd m⁻², respectively.^[60] The CIE coordinate migration (Δx, Δy) in such a broad range of bias conditions was less than (±0.009, ±0.005). High EQEs of up to 5.9% were obtained in these WLECs, in spite of some energy loss into side emission from CCLs (Table 1). This work demonstrated a feasible way to achieve stable white EL from WLECs.

4.2 WLECs Based on Phosphorescent Sensitized Fluorescence

Improvement in device efficiency of WLECs is impeded by the low PLQYs of the red-emitting CTMCs (<20%, even in dilute solutions) used in CTMC-based WLECs.^[52,53] Fluorescent LECs based on phosphorescent sensitization constitute an alternative way to reach efficiencies similar to those of phosphorescent LECs.^[56,66,67] In phosphorescent sensitized fluorescence,^[68] the heavy-metal center of the phosphorescent host facilitates rapid intersystem crossing for efficient intramolecular singlet-to-triplet energy transfer and, thus, subsequent effective Förster energy transfer^[69] from triplet excitons of the phosphorescent host to singlet excitons of the fluorescent guest, harvesting both singlet and triplet excitons in the host molecules. Hence, device efficiencies of phosphorescent sensitized fluorescent LECs can approach those of phosphorescent LECs. Since various efficient red-emitting fluorescent dyes^[70] (PLQYs > 90% in dilute solutions) are commercially available, phosphorescent sensitization is also a feasible way to achieve efficient host-guest WLECs. In 2012, Su et al. reported WLECs based on a blue-emitting phosphorescent CTMC (**C5B**), as the host, and a red-emitting fluorescent dye (Sulforhodamine 101), as the guest.^[71] Sulforhodamine 101 (**SR101**), as shown in Figure 11, is commercially available and exhibits a high PLQY of up to $95 \pm 2\%$ in solution.^[72] The maximal EQE achieved from the phosphorescent sensitized WLECs (mass ratio **C5B**:BMIMPF₆:**SR101** = 79.7:20:0.3) reached 7.9% (Table 1). Furthermore, the emissive layer thickness was properly chosen, such that the full width at half maximum of the blue EL emission was significantly reduced due to destructive interference of the green part of the emission spectrum in a microcavity device structure (Figure 12). Tailoring the output EL spectrum via the thickness-dependent microcavity effect is especially useful for enabling CTMC-based WLECs to achieve white EL with CIE coordinates approaching (0.33, 0.33), since saturated deep blue-emitting CTMCs are currently still scarce. Reported WLECs based on sky blue-emitting CTMCs generally exhibit greenish white EL, even when combined with saturated red CTMCs (cf. Figures 7 and 9). Without saturated deep blue-emitting

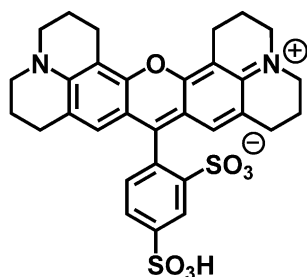


Figure 11. Molecular structure of the red-emitting fluorescent dye **SR101**.

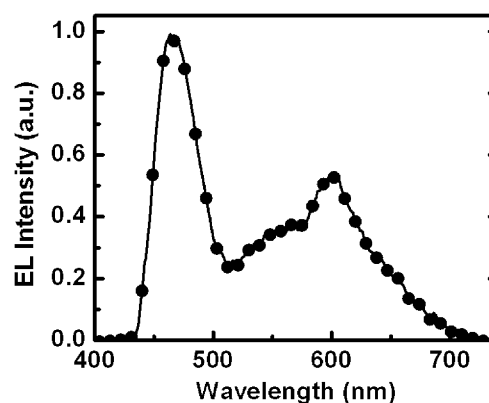


Figure 12. EL spectrum of phosphorescent sensitized WLEC (mass ratio **C5B**:BMIMPF₆:**SR101** = 79.7:20:0.3) under 3.6 V.

CTMCs, suppressing green emission of sky blue-emitting CTMCs by employing the microcavity effect represents a feasible way to obtain more saturated blue emission and, thus, purer white EL emission.

5 Summary and Outlook

This paper reviewed the development of WLECs based on conjugated polymers and CTMCs. White EL from polymer LECs was easily obtained by utilizing phase separation or excimer emission in a single-component emissive layer. To improve the spectral quality of white EL of polymer WLECs, an emissive layer with a properly adjusted mixing ratio of blue, green, and red-emitting copolymers was employed. Furthermore, polymer WLECs based on a single polymer with multiple chromophores were proposed to simplify device fabrication processes. Device efficiencies of fluorescent polymer WLECs were generally limited by spin statistics, and thus, WLECs based on phosphorescent CTMCs were reported to enhance EL efficiencies. In addition to typical WLECs based on host-guest CTMCs, a double-doping strategy and adjustment of the emissive layer thickness were proposed to improve carrier balance, rendering even higher device efficiencies. WLECs composed of red CCLs attached to blue-emitting LECs were demonstrated to improve temporal spectral stability of white EL. Since highly efficient fluorescent red-emitting dyes are commercially available, phosphorescent sensitized WLECs, based on a blue-emitting phosphorescent CTMC and a fluorescent red-emitting dye, were shown to exhibit high device efficiencies.

Enormous enhancement in device efficiencies of WLECs has been made in recent years thanks to the design and synthesis of efficient materials, most of them based on CTMCs. In addition, deeper understanding of device physics has facilitated improvement of the carrier balance of WLECs, resulting in further increased device

efficiencies. However, the state-of-the-art power efficiency of WLECs is ca. 20 lm W^{-1} ,^[64] which is still not adequate for solid-state lighting. Further improvement of PLOQs of emissive materials, especially for the red-emitting CTMCs, will be necessary to meet the requirements of applications. Moreover, the trade-off between device response and stability is an important issue for commercialization of WLECs. Pulsed-current driving of LECs was proposed to simultaneously obtain rapid turn-on and stable EL.^[41] Nevertheless, device characteristics of WLECs under pulsed-current driving should be further examined. Since higher-gap, blue-emitting CTMCs generally contain electron-withdrawing substituents (e.g., fluorine [cf. Figure 5]), they are typically much less stable than their lower-gap red counterparts.^[73] Detailed understanding of the processes of electrically driven chemical degradation of blue-emitting CTMCs is essential for synthesizing robust host materials for WLECs. In spite of challenges ahead, continuous improvements in device performance of WLECs is expected in the future, making them promising candidates for power-efficient lighting sources.

Acknowledgments

The authors gratefully acknowledge the financial support from the National Science Council of Taiwan.

References

- [1] J. Kido, K. Hongawa, K. Okuyama, K. Nagai, *Appl. Phys. Lett.* **1994**, *64*, 815–817.
- [2] B. W. D'Andrade, S. R. Forrest, *Adv. Mater.* **2004**, *16*, 1585–1595.
- [3] G. Zhou, W.-Y. Wong, S. Suo, *J. Photochem. Photobiol. C* **2010**, *11*, 133–156.
- [4] M. C. Gather, A. Köhnen, K. Meerholz, *Adv. Mater.* **2011**, *23*, 233–248.
- [5] B. Zhang, G. Tan, C.-S. Lam, B. Yao, C.-L. Ho, L. Liu, Z. Xie, W.-Y. Wong, J. Ding, L. Wang, *Adv. Mater.* **2012**, *24*, 1873–1877.
- [6] Q. Pei, G. Yu, C. Zhang, Y. Yang, A. J. Heeger, *Science* **1995**, *269*, 1086–1088.
- [7] Q. Pei, Y. Yang, G. Yu, C. Zhang, A. J. Heeger, *J. Am. Chem. Soc.* **1996**, *118*, 3922–3929.
- [8] M. Lenes, G. Garcia-Belmonte, D. Tordera, A. Pertegas, J. Bisquert, H. J. Bolink, *Adv. Funct. Mater.* **2011**, *21*, 1581–1586.
- [9] D. J. Dick, A. J. Heeger, Y. Yang, Q. Pei, *Adv. Mater.* **1996**, *8*, 985–987.
- [10] J. Gao, G. Yu, A. J. Heeger, *Appl. Phys. Lett.* **1997**, *71*, 1293–1295.
- [11] J. Gao, J. Dane, *Appl. Phys. Lett.* **2003**, *83*, 3027–3029.
- [12] Y. Hu, J. Gao, *Appl. Phys. Lett.* **2006**, *89*, 253514.
- [13] Y. Shao, G. C. Bazan, A. J. Heeger, *Adv. Mater.* **2007**, *19*, 365–370.
- [14] D. Hohertz, J. Gao, *Adv. Mater.* **2008**, *20*, 3298–3302.
- [15] J. Fang, P. Matyba, L. Edman, *Adv. Funct. Mater.* **2009**, *19*, 2671–2676.
- [16] A. Sandström, P. Matyba, L. Edman, *Appl. Phys. Lett.* **2010**, *96*, 053303.
- [17] S. van Reenen, P. Matyba, A. Dzwilewski, R. A. J. Janssen, L. Edman, M. Kemerink, *J. Am. Chem. Soc.* **2010**, *132*, 13776–13781.
- [18] X. Li, J. Gao, G. Liu, *Appl. Phys. Lett.* **2013**, *102*, 223303.
- [19] X. Li, J. Gao, G. Liu, *Org. Electron.* **2013**, *14*, 1441–1446.
- [20] J. K. Lee, D. S. Yoo, E. S. Handy, M. F. Rubner, *Appl. Phys. Lett.* **1996**, *69*, 1686–1688.
- [21] E. S. Handy, A. J. Pal, M. F. Rubner, *J. Am. Chem. Soc.* **1999**, *121*, 3525–3528.
- [22] F. G. Gao, A. J. Bard, *J. Am. Chem. Soc.* **2000**, *122*, 7426–7427.
- [23] H. Rudmann, M. F. Rubner, *J. Appl. Phys.* **2001**, *90*, 4338–4345.
- [24] F. G. Gao, A. J. Bard, *Chem. Mater.* **2002**, *14*, 3465–3470.
- [25] H. Rudmann, S. Shimada, M. F. Rubner, *J. Am. Chem. Soc.* **2002**, *124*, 4918–4921.
- [26] H. Rudmann, S. Shimada, M. F. Rubner, *J. Appl. Phys.* **2003**, *94*, 115–122.
- [27] J. Slinker, D. Bernards, P. L. Houston, H. D. Abruña, S. Bernhard, G. G. Malliaras, *Chem. Commun.* **2003**, 2392–2399.
- [28] J. D. Slinker, A. A. Gorodetsky, M. S. Lowry, J. J. Wang, S. Parker, R. Rohl, S. Bernhard, G. G. Malliaras, *J. Am. Chem. Soc.* **2004**, *126*, 2763–2767.
- [29] J. D. Slinker, C. Y. Koh, G. G. Malliaras, M. S. Lowry, S. Bernhard, *Appl. Phys. Lett.* **2005**, *86*, 173506.
- [30] A. R. Hosseini, C. Y. Koh, J. D. Slinker, S. Flores-Torres, H. D. Abruña, G. G. Malliaras, *Chem. Mater.* **2005**, *17*, 6114–6116.
- [31] A. B. Tamayo, S. Garon, T. Sajoto, P. I. Djurovich, I. M. Tsyba, R. Bau, M. E. Thompson, *Inorg. Chem.* **2005**, *44*, 8723–8732.
- [32] S. T. Parker, J. D. Slinker, M. S. Lowry, M. P. Cox, S. Bernhard, G. G. Malliaras, *Chem. Mater.* **2005**, *17*, 3187–3190.
- [33] Q. S. Zhang, Q. G. Zhou, Y. X. Cheng, L. X. Wang, D. G. Ma, X. B. Jing, F. S. Wang, *Adv. Funct. Mater.* **2006**, *16*, 1203–1208.
- [34] H.-C. Su, C.-C. Wu, F.-C. Fang, K.-T. Wong, *Appl. Phys. Lett.* **2006**, *89*, 261118.
- [35] H.-C. Su, F.-C. Fang, T.-Y. Hwu, H.-H. Hsieh, H.-F. Chen, G.-H. Lee, S.-M. Peng, K.-T. Wong, C.-C. Wu, *Adv. Funct. Mater.* **2007**, *17*, 1019–1027.
- [36] J. D. Slinker, J. Rivnay, J. S. Moskowitz, J. B. Parker, S. Bernhard, H. D. Abruña, G. G. Malliaras, *J. Mater. Chem.* **2007**, *17*, 2976–2988.
- [37] H. J. Bolink, E. Coronado, R. D. Costa, E. Ortí, M. Sessolo, S. Graber, K. Doyle, M. Neuberger, C. E. Housecroft, E. C. Constable, *Adv. Mater.* **2008**, *20*, 3910–3913.
- [38] H. J. Bolink, E. Coronado, R. D. Costa, N. Lardies, E. Ortí, *Inorg. Chem.* **2008**, *47*, 9149–9151.
- [39] C. H. Yang, J. Beltran, V. Lemaire, J. Cornil, D. Hartmann, W. Sarfert, R. Frohlich, C. Bizzarri, L. De Cola, *Inorg. Chem.* **2010**, *49*, 9891–9901.
- [40] C.-T. Liao, H.-F. Chen, H.-C. Su, K.-T. Wong, *J. Mater. Chem.* **2011**, *21*, 17855–17862.
- [41] D. Tordera, S. Meier, M. Lenes, R. D. Costa, E. Ortí, W. Sarfert, H. J. Bolink, *Adv. Mater.* **2012**, *24*, 897–900.
- [42] R. D. Costa, E. Ortí, H. J. Bolink, F. Monti, G. Accorsi, N. Armaroli, *Angew. Chem. Int. Ed.* **2012**, *51*, 8178–8211.

- [43] T. Hu, L. He, L. Duan, Y. Qiu, *J. Mater. Chem.* **2012**, *22*, 4206–4215.
- [44] N. M. Shavaleev, R. Scopelliti, M. Grätzel, M. K. Nazeeruddin, A. Pertegás, C. Roldán-Carmona, D. Tordera, H. J. Bolink, *J. Mater. Chem. C* **2013**, *1*, 2241–2248.
- [45] J.-S. Lu, J.-C. Kuo, H.-C. Su, *Org. Electron.* **2013**, *14*, 3379–3384.
- [46] Y. Yang, Q. Pei, *J. Appl. Phys.* **1997**, *81*, 3294–3298.
- [47] M. Sun, C. Zhong, F. Li, Y. Cao, Q. Pei, *Macromolecules* **2010**, *43*, 1714–1718.
- [48] S. Tang, J. Pan, H. Buchholz, L. Edman, *ACS Appl. Mater. Interfaces* **2011**, *3*, 3384–3388.
- [49] C. W. Tang, S. A. Van Slyke, C. H. Chen, *J. Appl. Phys.* **1989**, *65*, 3610–3616.
- [50] C.-S. Tsai, S.-H. Yang, B.-C. Liu, H.-C. Su, *Org. Electron.* **2013**, *14*, 488–499.
- [51] S. Tang, J. Pan, H. A. Buchholz, L. Edman, *J. Am. Chem. Soc.* **2013**, *135*, 3647–3652.
- [52] H.-C. Su, H.-F. Chen, F.-C. Fang, C.-C. Liu, C.-C. Wu, K.-T. Wong, Y.-H. Liu, S.-M. Peng, *J. Am. Chem. Soc.* **2008**, *130*, 3413–3419.
- [53] L. He, J. Qiao, L. Duan, G. F. Dong, D. Q. Zhang, L. D. Wang, Y. Qiu, *Adv. Funct. Mater.* **2009**, *19*, 2950–2960.
- [54] L. He, L. Duan, J. Qiao, G. Dong, L. Wang, Y. Qiu, *Chem. Mater.* **2010**, *22*, 3535–3542.
- [55] B. Chen, Y. Li, Y. Chu, A. Zheng, J. Feng, Z. Liu, H. Wu, W. Yang, *Org. Electron.* **2013**, *14*, 744–753.
- [56] C.-C. Ho, H.-F. Chen, Y.-C. Ho, C.-T. Liao, H.-C. Su, K.-T. Wong, *Phys. Chem. Chem. Phys.* **2011**, *13*, 17729–17736.
- [57] C.-T. Liao, H.-F. Chen, H.-C. Su, K.-T. Wong, *Phys. Chem. Chem. Phys.* **2012**, *14*, 1262–1269.
- [58] H.-F. Chen, C.-T. Liao, H.-C. Su, Y.-S. Yeh, K.-T. Wong, *J. Mater. Chem. C* **2013**, *1*, 4647–4654.
- [59] H.-C. Su, H.-F. Chen, Y.-C. Shen, C.-T. Liao, K.-T. Wong, *J. Mater. Chem.* **2011**, *21*, 9653–9660.
- [60] H.-B. Wu, H.-F. Chen, C.-T. Liao, H.-C. Su, K.-T. Wong, *Org. Electron.* **2012**, *13*, 483–490.
- [61] T.-W. Wang, H.-C. Su, *Org. Electron.* **2013**, *14*, 2269–2277.
- [62] X. Liu, D. Poitras, Y. Tao, C. Py, *J. Vac. Sci. Technol., A* **2004**, *22*, 764–767.
- [63] I. H. Campbell, D. L. Smith, C. J. Neef, J. P. Ferraris, *Appl. Phys. Lett.* **1998**, *72*, 2565–2567.
- [64] Y.-P. Jhang, H.-F. Chen, H.-B. Wu, Y.-S. Yeh, H.-C. Su, K.-T. Wong, *Org. Electron.* **2013**, *14*, 2424–2430.
- [65] A. R. Duggal, J. J. Shiang, C. M. Heller, D. F. Foust, *Appl. Phys. Lett.* **2002**, *80*, 3470–3472.
- [66] H.-C. Su, Y.-H. Lin, C.-H. Chang, H.-W. Lin, C.-C. Wu, F.-C. Fang, H.-F. Chen, K.-T. Wong, *J. Mater. Chem.* **2010**, *20*, 5521–5526.
- [67] C.-L. Lee, C.-Y. Cheng, H.-C. Su, *Org. Electron.* **2014**, *15*, 711–720.
- [68] M. A. Baldo, M. E. Thompson, S. R. Forrest, *Nature* **2000**, *403*, 750–753.
- [69] T. Förster, *Discuss. Faraday Soc.* **1959**, *27*, 7–17.
- [70] R. F. Kubin, A. N. Fletcher, *J. Lumin.* **1982**, *27*, 455–462.
- [71] H.-C. Su, H.-F. Chen, P.-H. Chen, S.-W. Lin, C.-T. Liao, K.-T. Wong, *J. Mater. Chem.* **2012**, *22*, 22998–23004.
- [72] R. A. Velapoldi, H. H. Tønnesen, *J. Fluoresc.* **2004**, *14*, 465–472.
- [73] D. Tordera, J. J. Serrano-Pérez, A. Pertegás, E. Ortí, H. J. Bolink, E. Baranoff, M. K. Nazeeruddin, J. Frey, *Chem. Mater.* **2013**, *25*, 3391–3397.

Received: February 13, 2014

Accepted: March 22, 2014

Published online: July 11, 2014